

Superparamagnetism and relaxation effects in granular Ni-SiO₂ and Ni-Al₂O₃ films

J. I. Gittleman, B. Abeles, and S. Bozowski

RCA Laboratories, Princeton, New Jersey 08540

(Received 19 October 1973)

The susceptibility of an array of fine nickel particles was measured as a function of temperature from 1.5 to 300 °K at a frequency of 5 kHz. The particles were formed by cosputtering nickel with SiO₂ or Al₂O₃ and varied in diameter between 10 and 100 Å. With increasing temperature, the susceptibility increased from its initial value to a maximum at a temperature T_B followed by a hyperbolic decrease. A theory based on the relaxation time for single-domain particles $\tau = \tau_0 e^{KV/kT}$ (K is the anisotropy energy, V is the particle volume) quantitatively explains the data. At $T = 0$ all the particles are blocked by the anisotropy barriers. As the temperature is increased the susceptibility increases because particles for which $\omega\tau < 1$ (ω is the angular frequency) are no longer blocked. Above T_B all the particles are unblocked and the susceptibility is characteristic of superparamagnetism. Analysis of the data yields information about the particle volume distribution function and a value for the effective anisotropy energy.

I. INTRODUCTION

The magnetic behavior of systems consisting of isolated, single-domain ferromagnetic particles depends on the relative magnitude of the thermal energy with respect to KV , where V is the particle volume and K the magnetic anisotropy energy. When $kT \gg KV$, the magnetization vector of a particle can rotate in response to a change in temperature or applied field and the superparamagnetic¹ thermal equilibrium is established within a very short time ($\sim 10^{-10}$ sec). When $kT \ll KV$ the presence of the anisotropy barrier impedes the rotation of the magnetization vectors and the system approaches equilibrium with a characteristic relaxation time² τ . When τ is much longer than the measuring time, the equilibrium state cannot be observed. The temperature below which this condition occurs has been referred to as the blocking temperature.² Relaxation effects have been studied in a system consisting of ferromagnetic precipitates in nonmagnetic metal matrices,³ Cu (2.0-at. % Co). However, no such studies have been made for small ferromagnetic metal particles in a dielectric matrix where all but magnetic dipole interactions are eliminated.

The purpose of the present work is the study of superparamagnetism and relaxation effects in granular metals consisting of small isolated ferromagnetic particles embedded in amorphous SiO₂ and Al₂O₃. The Ni-SiO₂ and Ni-Al₂O₃ systems were selected for study since extensive work has already been done on their magnetic^{4,5} and electrical transport^{4,6} properties and on their microstructure.^{7,8} In Fig. 1 are shown the ordering temperature^{4,5} T'_c and the electrical resistivity⁴ ρ vs vol-% of SiO₂ in the Ni-SiO₂ system. T'_c is the temperature at which the magnetic moments of adjacent grains order. The abrupt decrease in T'_c and the correspondingly abrupt in-

crease in ρ near the 50-vol% composition is associated with a transition in the microstructure from a continuous metal phase to one of isolated nickel particles dispersed in amorphous SiO₂. It is the compositional range for which the Ni concentration is less than 50 vol% that is the subject of the present work. Measurements were made of the magnetic susceptibility of sputtered granular films at 5 kHz in the temperature range 1.5–300 °K. The results are explained on the basis of a simple model of the superparamagnetic granular metal.

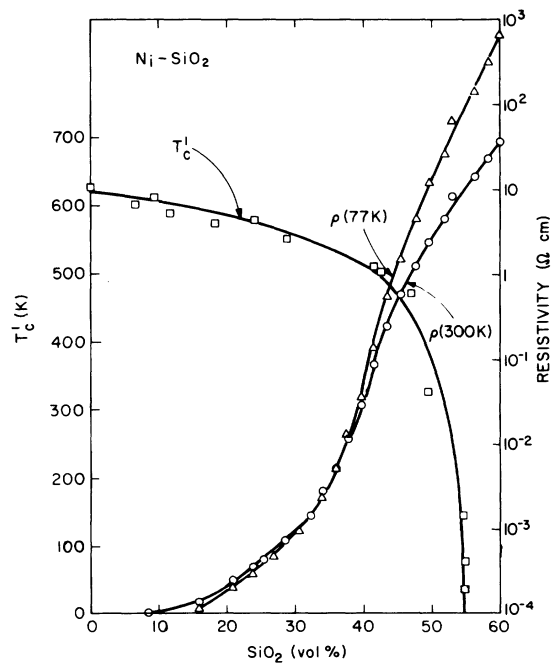


FIG. 1. Ordering temperature T'_c and resistivity ρ at 300 and 77 °K vs vol-% SiO₂ in the Ni-SiO₂ system.

II. EXPERIMENTAL

The granular metal films about $2 \mu\text{m}$ thick were prepared by rf sputtering at a pressure of 4×10^{-3} -Torr argon from composite targets of Ni and dielectric. The composite targets were made by placing a $\frac{1}{16}$ -in.-thick silica (SiO_2) or alumina (Al_2O_3) plate of the appropriate shape on top of a 6-in.-diam Ni disk. The substrates were sapphire or Pyrex 0.090 in. wide, 0.10 in. long, and 0.010 in. thick, and were mounted on a water-cooled substrate holder at a height of 2.3 in. above the target. The sputtering rates were about $0.5 \mu\text{m}/\text{h}$. The composition of a specimen was determined by its position with respect to the sputtering target, being metal rich at the end facing the metallic part of the target and insulator rich in the region facing the part of the target covered by insulator. The compositions of the film were determined from the measured thickness of the films using the method of Hanak.⁹ This method of compositional determination yielded an estimated accuracy of about ± 10 -vol% Ni. Even though the absolute values of the compositions are not known accurately, the differences in the composition of samples made during the same sputtering run are known very accurately.⁹ More details on the preparation of the films are given elsewhere.⁸

A. Microstructure of films

The transmission electron microscopy studies were made with a Philips EM300 electron microscope having a resolution of about 2 \AA . Ni-SiO₂ films were sputtered onto carbon films mounted on a copper mesh. An electron micrograph of a Ni-SiO₂ film containing 40-vol% Ni is shown in Fig. 2. The average grain size is about 35 \AA . The electron diffraction patterns differed from those of bulk crystalline nickel only in that the lines were broadened due to the small size of the nickel particles. The measured lattice constant was $a_0 = 3.52 \pm 0.01 \text{ \AA}$, which agrees within experimental error with the bulk value. The same lattice constant was also obtained with x rays on $2\text{-}\mu\text{m}$ -thick Ni-SiO₂ films deposited on glass. In contrast to our results, Abrahams *et al.*⁷ reported a large lattice expansion for their Ni-SiO₂ films. Apart from the fact that their films were prepared in a different sputtering system, we have at present no satisfactory explanation for the large discrepancy in the lattice constants obtained by the two groups.

B. Magnetic measurements

The susceptibility of the specimens was measured using a balanced mutual inductance bridge. Two identical pickup coils were connected in series opposition and immersed in an ac magnetic field having a frequency of 5 kHz and 2 Oe amplitude.

The signal obtained when a specimen is moved from one coil to the other coil is proportional to the initial susceptibility of the specimen and was measured with a PAR-HR8 lock-in detector. The bridge was calibrated by measuring the signal of a specimen with a known susceptibility. The axis of the pick-up coils and the direction of the ac magnetic field were parallel to each other and were in the plane of the film.

III. THEORY

We calculate the temperature dependence of the susceptibility of an array of isolated ferromagnetic particles using the following simple model: (i) The Curie temperature of each particle is high compared to the temperature T , and the magnetization M_s of the particle is independent of temperature. (ii) The relaxation time τ is given by²

$$\tau = \tau_0 \exp(E_B/kT) \quad , \quad (1a)$$

where τ_0 is a slowly varying function of temperature and is of the order of $10^{-10} \text{ sec}^{2,10,11}$ and E_B is the anisotropy barrier height given by²

$$E_B = KV \quad (1b)$$

for uniaxial anisotropy,

$$E_B = \frac{1}{4} K_1 V \quad (1c)$$

for cubic anisotropy ($K_1 > 0$), and

$$E_B = \frac{1}{12} |K_1| V \quad (1d)$$

for cubic anisotropy ($K_1 < 0$). (iii) It is assumed that there is a distribution in the volumes of the particles and that the susceptibility of the system is given by

$$\chi(T, \omega) = \int_0^\infty \chi_V(T, \omega) f(V) dV \quad , \quad (2)$$

where $f(V)$ is the volume distribution function, ω is the angular frequency, and $\chi_V f(V) dV$ is the contribution to the total susceptibility of particles with volumes in the range dV about V . (iv) The form of $\chi_V(\omega, T)$ is deduced using the following simple physical argument. Assume that the external magnetic field is a step function of amplitude H_0 turned on at

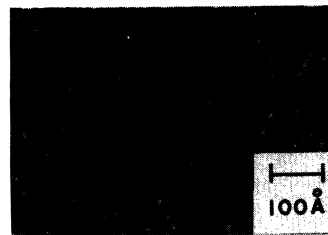


FIG. 2. Electron micrograph of Ni-SiO₂ film containing 40-vol% Ni.

time $t=0$. The contribution $M_V(t)$ of the particles with volume V to the total magnetization is given by

$$M_V(t) = H_0 [\chi_0 - (\chi_0 - \chi_1) e^{-t/\tau}] , \quad (3)$$

where χ_0 is the superparamagnetic susceptibility corresponding to thermal equilibrium given by¹

$$\chi_0 = M_s^2 V x / 3kT , \quad (4)$$

x is the volume fraction occupied by the ferromagnetic particles, χ_1 is the susceptibility of collection of single domain particles² responding to the external field and the magnetic anisotropy and is given by¹²

$$\chi_1 = a M_s^2 x / |K| , \quad (5)$$

where $a = \frac{1}{2} \langle \sin^2 \theta \rangle$, θ is the angle between the applied field and the easy direction of magnetization and the average is over all particles. When the susceptibility is given by Eq. (5) we refer to the system as being in a "blocked" state.

The underlying physical process described by Eq. (3) is that in response to an external field in the form of a step function, the system acquires a magnetization appropriate to Eq. (5) in a time short compared to τ . Subsequently, the system relaxes via thermal fluctuations to the superparamagnetic state characterized by a susceptibility given by Eq. (4). The Fourier transform of Eq. (3) leads to a complex susceptibility

$$\tilde{\chi} = (\chi_0 + i\omega\tau\chi_1) / (1 + i\omega\tau) , \quad (6)$$

whose real part is given by

$$\chi_V(\omega, T) = (\chi_0 + \omega^2\tau^2\chi_1) / (1 + \omega^2\tau^2) . \quad (7)$$

Equation (7) reduces to the expression used by Jordan³ if we set $\chi_1 = 0$. However $\chi_1 = 0$ precludes the existence of a blocked state.

Substituting Eqs. (6) and (1) into Eq. (2) leads to the general form for $\chi(T, \omega)$. Explicit forms of Eq. (2) are derived for the high- and low-temperature limits in the Appendix. In the high-temperature limit $kT \gg K\bar{V}$

$$\chi(\omega, T) = M_s^2 \bar{V} x / 3kT \quad (8)$$

and

$$\bar{V} = \int_0^\infty V f(V) dV , \quad (9)$$

where \bar{V} is the average volume. In the low-temperature limit $kT \ll K\bar{V}$ only particles whose volume $V \ll \bar{V}$ contribute to the temperature-dependent part of the susceptibility. If in the limit $V \rightarrow 0$ the dominant term in $f(V)$ is V^n , we obtain from Eq. (2),

$$\chi(\omega, T) = \chi_1 (1 + AT^{n+1}) . \quad (10)$$

The susceptibility given by Eq. (2) exhibits a maximum. The temperature T_B at which the max-

imum occurs depends on the form of $f(V)$. In the Appendix we have calculated expressions for T_B corresponding to three special distribution functions: the rectangular distribution function

$$f(V) = 1/2\bar{V} , \quad V \leq 2\bar{V} \\ = 0 , \quad V > 2\bar{V} , \quad (11)$$

for which

$$T_B = 2K\bar{V}/k |\ln \omega\tau_0| ; \quad (12)$$

the Poisson distribution function

$$f(V) = (4V/\bar{V}^2) e^{-2V/\bar{V}} , \quad (13)$$

for which

$$T_B = 1.8K\bar{V}/k |\ln \omega\tau_0| ; \quad (14)$$

and a δ -function distribution

$$f(V) = \delta(V - \bar{V}) , \quad (15)$$

for which

$$T_B = K\bar{V}/k |\ln \omega\tau_0| . \quad (16)$$

Equations (12), (14), and (16) apply to the case of uniaxial unisotropy. In the case of cubic anisotropy K is replaced by $\frac{1}{4}K_1$ for $K_1 > 0$ and $\frac{1}{12}|K_1|$ for $K_1 < 0$.

IV. DISCUSSION

In Figs. 3 and 4 are shown plots of initial susceptibility χ vs temperature T for several Ni-SiO₂ and Ni-Al₂O₃ films. In general, the susceptibility rises with increasing temperature to a maximum at a temperature, T_B . Above T_B the susceptibility falls hyperbolically. T_B is a function of composition and increases in value with increasing nickel concentration. It is convenient to divide the analysis into two temperature regimes, $T > T_B$ and $T < T_B$.

The reciprocal susceptibility plotted as a function of temperature can be fitted by a Curie law for $T > T_B$ over a wide temperature range for specimens containing less than about 50-vol% Ni. A typical example of this behavior is given in Fig. 5. Figure 6 is a similar plot for a Ni-SiO₂ specimen containing 52-vol% Ni. The high-temperature data exhibit Curie-Weiss behavior with an ordering temperature of about 22 °K, suggesting the onset of interparticle interactions at this composition. The departure from the linear behavior at high temperatures (seen in Figs. 5 and 6) is probably due to the temperature dependence of M_s .¹³

The slope of the reciprocal susceptibility, in the high-temperature region, together with Eq. (8) were used to determine the mean particle volume \bar{V} . The published value¹⁴ for M_s 509 emu and the nominal compositions x (see Sec. II) were used in Eq. (8). In Table I are given the compositions, the observed values of T_B , and the calculated values of \bar{V} for all the granular Ni films studied. The

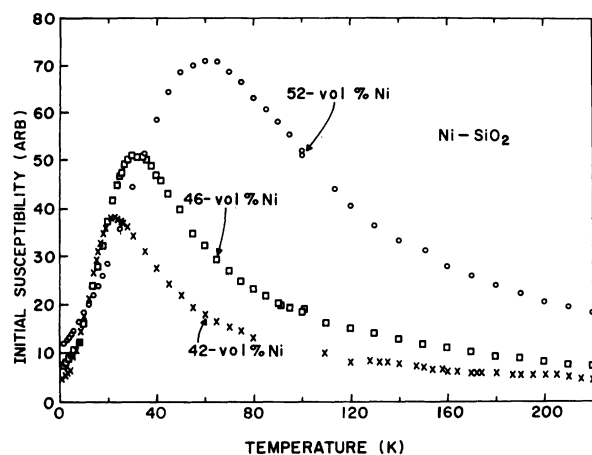


FIG. 3. Initial susceptibility vs temperature for Ni-SiO₂ films.

electron microscopy indicates a broad distribution function $f(V)$ making direct determination of \bar{V} difficult. However, a rough estimate of the mean size of the Ni particles in the Ni-SiO₂ films is in reasonable agreement with the values given in Table I. According to Table I the mean volumes of the Ni particles in the Ni-Al₂O₃ films appear to be generally larger than those in the Ni-SiO₂ films of the same composition. However, we lack direct evidence for this difference. We do not have available electron micrographs for the Ni-Al₂O₃ films and furthermore there is a larger uncertainty in the concentration of the Al₂O₃ than the SiO₂ (see Sec. II).

As shown in Sec. III, the temperature dependence of χ at low temperatures ($T \ll T_B$) yields informa-

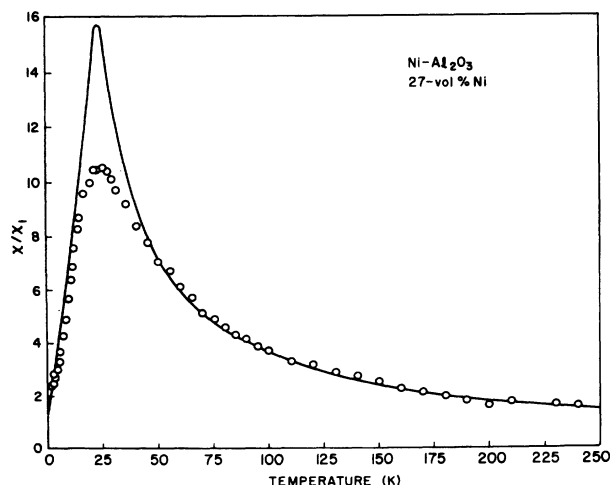


FIG. 4. Initial susceptibility vs temperature for Ni-Al₂O₃ film. The curve was computed from Eqs. (2) and (7) using $\bar{V} = 4.3 \times 10^{-20}$ cm³, $K = 4.5 \times 10^5$ erg/cm³ and $\alpha = 0.13$.

TABLE I. Nominal compositions, observed values of T_B , and calculated values of \bar{V} for all the granular Ni films studied.

Insulator	Nickel Concentration (vol%)	\bar{V}^a 10 ⁻²⁰ cm ³	T_B^b K	K^c 10 ⁻⁵ erg/cm ³
SiO ₂	38	3.15	18	4.6
	42	4.37	23	4.1
	46	6.41	35	4.3
	52	12.1	62	4.1
Al ₂ O ₃	27	4.25	22	4.5
	32	7.45	34	4.0
	36	12.9	52	3.5

^aCalculated using high-temperature data and Eq. (8).

^bExperimental values.

^cCalculated using Eq. (14) for Ni-SiO₂ and Eq. (12) for Ni-Al₂O₃ with $\tau_0 = 10^{-10}$ sec.

tion about particle volume distribution $f(V)$. Specifically the value of n in Eq. (10) determines the power law of $f(V)$ for small V . The low temperature susceptibilities for the Ni-Al₂O₃ specimens can best be fitted by a linear temperature dependence ($n=0$), as shown in Fig. 7. On the other hand, the data for the Ni-SiO₂ specimens are best fitted by a T^2 law ($n=1$) as shown in Fig. 8. Thus for $V \ll \bar{V}$, $f(V) = \text{const.}$ for the Ni-Al₂O₃ system and $f(V) \propto V$ for the Ni-SiO₂ system. The distribution function used by Sheng *et al.*⁶ for describing the transport properties is equivalent to setting $n = -\frac{1}{3}$. This value of n is inconsistent with our low-temperature data. However, the fit to their experimental data is insensitive to the detailed shape of the distribution function, provided it is broad.

In the last column of Table I are given values of the anisotropy energy K computed from the observed values of T_B and the computed value of \bar{V} . We have used Eq. (12) for the Ni-Al₂O₃ and Eq. (14) for the Ni-SiO₂. It should be noted however that, as long as the distribution function $f(V)$ is broad, the calculated value of K is not sensitive to the specific form of the function. The magnitudes of K are relatively independent of type and concen-

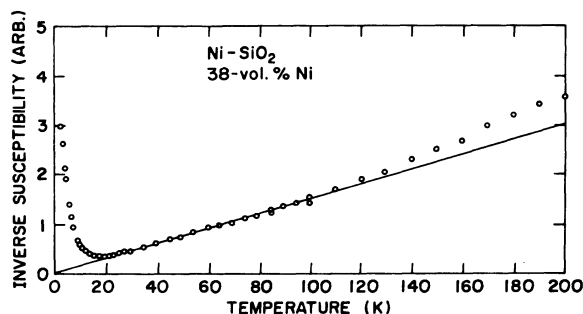


FIG. 5. Reciprocal susceptibility vs temperature for 38-vol% Ni in Ni-SiO₂.

tration of the insulator and its average value is 4.2×10^5 ergs/cm³.

The solid curve in Fig. 4 was computed using Eqs. (2) and (7). Because of the linear low-temperature dependence of susceptibility exhibited by Ni-Al₂O₃ specimens, the distribution function was assumed given by Eq. (11). Values of \bar{V} and K were taken to be 4.3×10^{-20} cm³ and 4.5×10^5 ergs/cm³, respectively (see Table I). The value of a was computed from the value of χ at $T=0$ and Eq. (5) to be 0.13. If we assume a rectangular distribution and compute a from $(1/\chi)(d\chi/dT)$ [see Appendix, Eq. (A7)], we get $a=0.17$. The value of 0.17 yields somewhat better agreement with the low-temperature data because its determination from the normalized slope does not require knowledge of α and of the absolute value of χ . The largest discrepancy between experiment and theory is the value of the susceptibility at T_B . Better agreement can be obtained by treating $\omega\tau_0$ as an adjustable parameter. However, without more information regarding $f(V)$, an exercise in parameter adjusting did not seem justified.

The values of K given in Table I are based on the assumption of uniaxial anisotropy. If we assume cubic anisotropy the average values of the anisotropy constants are $K_1 = -5 \times 10^6$ ergs/cm³ or $K_1 = +1.6 \times 10^6$ ergs/cm³. The value of K_1 for Ni at low temperatures is¹⁵ -7.5×10^5 ergs/cm³. It thus appears that crystalline anisotropy cannot explain the large barrier in small Ni particles. Other likely sources of magnetic anisotropy are shape anisotropy and strain anisotropy, which are uniaxial. To account for a uniaxial anisotropy of $K=4.2 \times 10^5$ requires, in the case of shape anisotropy, rod-shaped particles with an aspect ratio of about 2:1, and, in the case strain anisotropy, a strain of 4×10^{-3} .

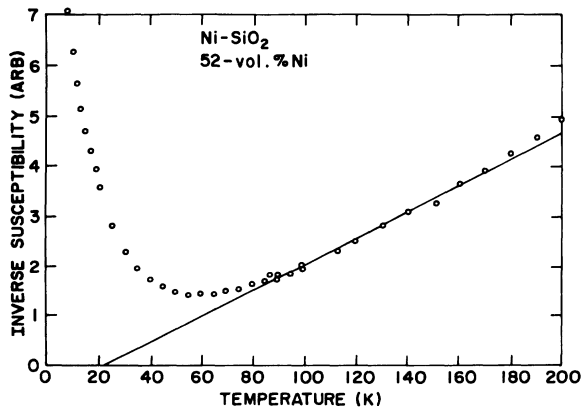


FIG. 6. Reciprocal susceptibility vs temperature for 52-vol% Ni in Ni-SiO₂.

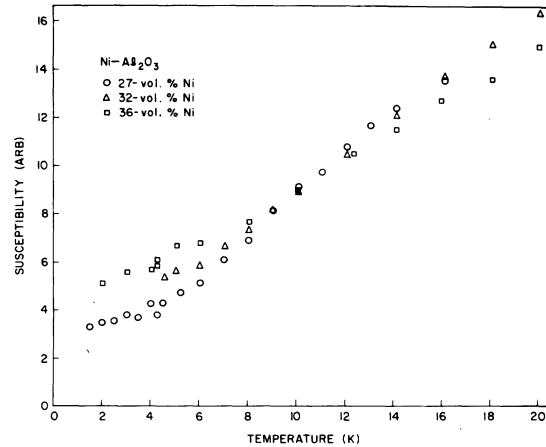


FIG. 7. Initial susceptibility of Ni-Al₂O₃ specimens vs T .

In conclusion, the magnetic susceptibility of granular Ni-SiO₂ and Ni-Al₂O₃ films containing less than 50 vol% Ni behaves like that of a system of isolated single domain particles. Mean-particle volumes determined from the temperature dependence of the susceptibility above T_B are consistent with estimates made from electron micrographs. It is of interest to estimate the lower limit of particle volume for the existence of ferromagnetism. Since the temperature dependence of χ for $T \ll T_B$ arises from particles for which $V \ll \bar{V}$ a broad size distribution of particles is required and particles with volumes appreciably smaller than the average are ferromagnetic. Thus, for the specimen containing 27-vol% Ni in Ni-Al₂O₃, \bar{V} was 3×10^{-20} cm³, corresponding to an average dimension of about 30 Å. Therefore, below room temperature, Ni particles which are considerably smaller than 30 Å are ferromagnetically ordered.

ACKNOWLEDGMENTS

It is a pleasure to thank R. W. Cohen for many illuminating discussions. We are also thankful to P. J. Wojtowicz for helpful comments, to Y. Arie for sample preparation and to M. Coutts for the electron microscopy and the x-ray studies. We would also like to thank Dr. A. E. Berkowitz for suggesting the simple model referred to earlier.

APPENDIX

In the following, we shall derive expressions for the high- and low-temperature values of $\chi(T)$ and for T_B , the temperature at the susceptibility maximum. Using Eqs. (1a), (1b), (2), (4), (5), and (7), the real part of the susceptibility can be written

$$\chi(T, \omega) = \chi_1 \int_0^\infty \frac{(KV/3akT) + \omega^2 \tau_0^2 e^{2KV/kT}}{1 + \omega^2 \tau_0^2 e^{2KV/kT}} f(V) dV. \quad (\text{A1})$$

In the present work the condition $\omega^2\tau_0^2 \ll 1$ ($\omega\tau_0 \sim 3 \times 10^{-6}$) is always fulfilled. In any system of particles there exists a maximum particle volume V_m . When $kT \geq KV_m$, the second term in both numerator and denominator of the integrand of Eq. (A1) can be neglected and

$$\begin{aligned}\chi(T, \omega) &= \chi_1 \frac{K}{3akT} \int_0^\infty Vf(V) dV \\ &= M_s^2 \bar{V} x / 3kT, \quad (\text{A2})\end{aligned}$$

the superparamagnetic value.

In general, Eq. (A1) can be written

$$\frac{\chi(T, \omega)}{\chi_1} = 1 + \int_0^\infty \left(\frac{KV}{3akT} - 1 \right) F\left(\frac{2KV}{kT} \right) f(V) dV, \quad (\text{A3})$$

where $F(y) = (1 + \omega^2\tau_0^2 e^y)^{-1}$. The function $F(y)$ resembles the Fermi function and because of the smallness of $\omega\tau_0$ is nearly rectangular. To a good approximation

$$\begin{aligned}F(y) &= 1 \quad y < 2|\ln\omega\tau_0| \\ &= 0, \quad y > 2|\ln\omega\tau_0|.\end{aligned} \quad (\text{A4})$$

Therefore,

$$\frac{\chi(T, \omega)}{\chi_1} = 1 + \int_0^{(kT/K)|\ln\omega\tau_0|} \left(\frac{KV}{3akT} - 1 \right) f(V) dV. \quad (\text{A5})$$

The physics implied by Eq. (A5) may be summarized as follows. At any temperature T , those particles whose volumes are less than $(kT/K)|\ln\omega\tau_0|$ are superparamagnetic and achieve thermal equilibrium in times short compared with ω^{-1} . On the other hand, particles whose volumes are greater than $(kT/K)|\ln\omega\tau_0|$ are effectively blocked from achieving thermal equilibrium¹⁶ during one period. Equation (A5) is a good approximation to the susceptibility over the whole temperature range.

When kT is sufficiently large compared with $K\bar{V}/|\ln\omega\tau_0|$, the upper limit can be replaced by infinity and superparamagnetism [Eq. (A2)] is obtained.

It can be seen directly from Eq. (A1) that $\lim_{T \rightarrow 0} \chi(T, \omega) = \chi_1$ as $T \rightarrow 0$, independent of the form of $f(V)$. However, the manner in which $\chi(T, \omega)$ approaches χ_1 does depend on $f(V)$. Thus if $f(V) = \delta(V - \bar{V})$, it follows directly from Eq. (A5) that

$$\begin{aligned}\chi(T, \omega) &= \chi_1 \quad \text{for } T < K\bar{V}/k|\ln\omega\tau_0| \\ &= M_s^2 \bar{V} x / 3kT \quad \text{for } T > K\bar{V}/k|\ln\omega\tau_0|.\end{aligned} \quad (\text{A6})$$

If

$$\begin{aligned}f(V) &= 1/2\bar{V} \quad \text{for } V < 2\bar{V} \\ &= 0 \quad \text{for } V > 2\bar{V}\end{aligned}$$

then, from Eq. (A5),

$$\chi(T, \omega) = \chi_1 \left[1 + \left(\frac{|\ln\omega\tau_0|}{2K\bar{V}} \right) \left(\frac{|\ln\omega\tau_0| - 1}{6a} \right) kT \right] \quad (\text{A7})$$

for $kT < 2K\bar{V}/|\ln\omega\tau_0|$. If $f(V) = (4V/\bar{V}^2) e^{-2V/\bar{V}}$, Eq. (A5) gives

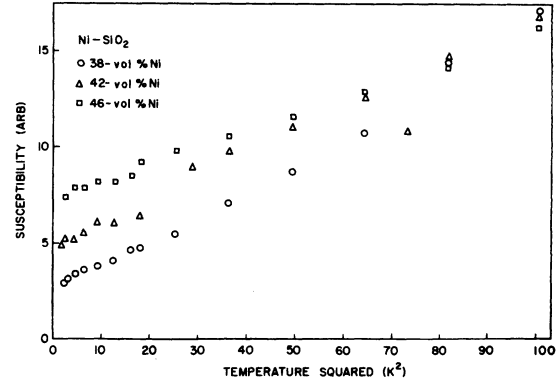


FIG. 8. Initial susceptibility of Ni-SiO₂ specimens vs T^2 .

$$\chi(T, \omega) = \chi_1 \left[1 + \frac{2|\ln\omega\tau_0|^2}{K^2 \bar{V}^2} \left(\frac{2|\ln\omega\tau_0|}{9a} - 1 \right) k^2 T^2 \right] \quad (\text{A8})$$

for $kT \ll K\bar{V}/2|\ln\omega\tau_0|$. It can also be shown readily from Eq. (A5) that if

$$\lim_{V \rightarrow 0} f(V) = \text{const } V^n,$$

then

$$\chi(T, \omega) = \chi_1 (1 + AT^{n+1} + \dots) \quad (\text{A9})$$

for $kT \ll K\bar{V}/|\ln\omega\tau_0|$, where A is a positive constant for $|\ln\omega\tau_0| > 3a(n+2)/(n+1)$. Since $\int_0^{V_1} f(V) dV$ is finite for any V_1 , n must be greater than -1 . Therefore it follows from Eq. (A9) that at low temperatures χ is an increasing function of temperature. At sufficiently high temperatures the system is superparamagnetic and χ is a decreasing function of temperature. Therefore there is a temperature T_B for which χ has a maximum value. From Eq. (A3) the susceptibility has a maximum when

$$G(T) \equiv \chi/\chi_1 - 1 = \int_0^\infty \left(\frac{K\bar{V}}{3akT} - 1 \right) F\left(\frac{2K\bar{V}}{kT} \right) f(V) dV \quad (\text{A10})$$

is a maximum. For the case $f(V) = \delta(V - \bar{V})$,

$$\begin{aligned}G(T) &= \left(\frac{K\bar{V}}{3akT} - 1 \right) F\left(\frac{2K\bar{V}}{kT} \right) \\ &\approx \frac{K\bar{V}}{3akT} - 1 \quad \text{for } T > \frac{K\bar{V}}{k|\ln\omega\tau_0|} \\ &\approx 0 \quad \text{for } T < \frac{K\bar{V}}{k|\ln\omega\tau_0|}.\end{aligned} \quad (\text{A11})$$

Therefore, $T_B = K\bar{V}/k|\ln\omega\tau_0|$. For the rectangular distribution function of Eq. (11),

$$\begin{aligned}G(T) &\approx \frac{K\bar{V}}{3akT} - 1 \quad \text{for } T > \frac{2K\bar{V}}{k|\ln\omega\tau_0|} \\ &\approx \frac{|\ln\omega\tau_0|}{2} \left(\frac{|\ln\omega\tau_0| - 1}{6a} \right) \frac{kT}{K\bar{V}} \quad \text{for } T < \frac{2K\bar{V}}{k|\ln\omega\tau_0|}.\end{aligned} \quad (\text{A12})$$

Since $|\ln\omega\tau_0| > 6a$, $G(T)$ is an increasing function of temperature for $T < 2K\bar{V}/k|\ln\omega\tau_0|$ and a decreasing function for $T > 2K\bar{V}/k|\ln\omega\tau_0|$. Thus

$$T_B = 2K\bar{V}/k|\ln\omega\tau_0| \quad (A13)$$

In the case of a Poisson's distribution, using Eq. (A5),

$$\frac{\chi(T, \omega)}{\chi_1} = 1 + \frac{4}{\bar{V}^2} \int^{(kT/K)|\ln\omega\tau_0|} \left(\frac{KV}{3akT} - 1 \right) V e^{-2V/\bar{V}} d\bar{V}. \quad (A14)$$

Putting $x = 2V/\bar{V}$, $\mu(\bar{t}) = \chi/\chi_1$ and $\bar{t} = 2k|\ln\omega\tau_0|T/K\bar{V}$, Eq. (A14) becomes after integration

$$\mu(\bar{t}) = A \left\{ \frac{1}{\bar{t}} - \left[\frac{1}{\bar{t}} + 1 - \frac{1}{A} + \left(\frac{1}{2} - \frac{1}{A} \right) \bar{t} \right] e^{-\bar{t}} \right\}, \quad (A15)$$

where $A = \frac{2}{3} |\ln\omega\tau_0|/a$. The susceptibility maximum is found by setting $d\mu/d\bar{t} = 0$ and solving for \bar{t} . Assuming $A^{-1} \ll 1$, the Newton-Raphson method yields a value of 3.6 for \bar{t} at the maximum so that

$$T_B = 1.8K\bar{V}/k|\ln\omega\tau_0|, \quad (A16)$$

only slightly different from the case of a rectangular distribution function [Eq. (A13)].

¹L. Neel, C. R. Acad. Sci. (Paris) 228, 604 (1949); C. P. Bean, J. Appl. Phys. 26, 1381 (1955).

²I. S. Jacobs and C. P. Bean, *Magnetism*, edited by G. T. Rado and H. Suhl (Academic, New York, 1963), Vol. III, pp. 271-294. C. P. Bean and J. D. Livingston, J. Appl. Phys. 30, 120S (1959).

³A. G. Jordan, Intern. J. Magn. 2, 123 (1972).

⁴J. I. Gittleman, Y. Goldstein, and S. Bozowski, Phys. Rev. B 5, 3609 (1972).

⁵M. Rayl, P. J. Wojtowicz, M. S. Abrahams, R. L. Harvey, and C. J. Buiocchi, Phys. Lett. A 36, 477 (1971).

⁶Ping Sheng and B. Abeles, Phys. Rev. Lett. 28, 34 (1972); Ping Sheng, B. Abeles, and Y. Arie, Phys. Rev. Lett. 31, 44 (1973).

⁷M. S. Abrahams, C. J. Buiocchi, M. Rayl, and P. J. Wojtowicz, J. Appl. Phys. 43, 2537 (1972).

⁸B. Abeles, Ping Sheng, Y. Arie, and M. Coutts (unpublished).

⁹J. J. Hanak, H. W. Lehman, and R. K. Wehner, J. Appl. Phys. 43, 1666 (1972).

¹⁰W. F. Brown, Jr., Phys. Rev. 130, 1677 (1963).

¹¹A. Aharoni, Phys. Rev. B 7, 1103 (1973).

¹²S. Chikazumi, *Physics of Magnetism* (Wiley, New York, 1964), p. 263.

¹³R. W. Cohen, M. Rayl, and B. Abeles (unpublished).

¹⁴R. M. Bozorth, *Ferromagnetism* (Van Nostrand, Princeton, N. J., 1951), p. 270.

¹⁵Reference 14, p. 569.

¹⁶This simplified model was first suggested to us by A. E. Berkowitz (private communication.)

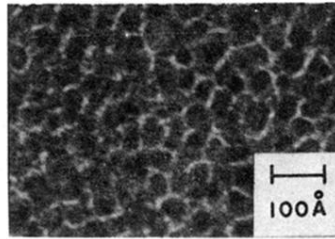


FIG. 2. Electron micrograph of Ni-SiO₂ film containing 40-vol% Ni.